A Suite of Triple Resonance NMR Experiments for the Backbone Assignment of ^{15}N, ^{13}C, ^{2}H Labeled Proteins with High Sensitivity

Toshio Yamazaki,[†,*] Weontae Lee,[‡] Cheryl H. Arrowsmith,[‡] D. R. Muhandiram,[†] and Lewis E. Kay[†,*]

Contribution from the Protein Engineering Centers of Excellence and Departments of Medical Genetics, Biochemistry, and Chemistry, University of Toronto, Toronto, Ontario, Canada M5S 1A8, and Division of Molecular and Structural Biology, Ontario Cancer Institute and Department of Medical Biophysics, University of Toronto, 500 Sherbourne Street, Toronto, Ontario, Canada M4X 1K9

Received July 18, 1994[⊗]

Abstract: A suite of NMR pulse schemes is presented for the assignment of HN, ^{15}N, $^{13}C^{\alpha}$, and $^{13}C^{\beta}$ resonances in ^{15}N, ^{13}C, ^{2}H labeled proteins. The experiments exploit the line narrowing of the ^{13}C spins caused by the substitution of deuterons for bound protons and are therefore well suited for application to molecules with masses on the order of 30−40 kDa where standard triple resonance experiments may fail completely or provide spectra of poor sensitivity. The methods are demonstrated on a 37 kDa ternary complex of a ^{15}N, ^{13}C, and ~70% ^{2}H labeled sample of trp-repressor, the corepressor 5-methyltryptophan, and a 20 basepair trp-operator DNA fragment. All of the experiments in the family presented provide well over 95% of the expected intra- and/or inter-residue correlations. Carbon relaxation measurements of the complex indicate that the use of deuteration increases the average $^{13}C^{\alpha}$ T_2 value from 16.5 to 130 ms.

Introduction

The development of triple resonance multidimensional NMR spectroscopy has greatly increased the scope of proteins that can be studied by NMR methods.[1,2] The basic building block of a triple resonance experiment consists of a set of pulses and delays during which magnetization is transferred between heteronuclei/homonuclei via the scalar coupling connecting the participating spins.[3,4] Because such couplings are considerably larger than homonuclear $^{1}H-^{1}H$ scalar couplings, the method can be applied to proteins which are significantly larger than would otherwise be possible using conventional ^{1}H NMR techniques. Nevertheless, the application of some of the triple resonance experiments to proteins on the order of 40 kDa can still pose a significant challenge due in large part to short transverse relaxation times which limit the transfer efficiency between coupled spins.

In the past years, a number of studies involving selective deuteration or perdeuteration of proteins in concert with 2D $^{1}H-^{1}H$ spectroscopy or ^{15}N-edited experiments have demonstrated the potential for sensitivity enhancement through the elimination of competing relaxation pathways that would otherwise be available to proton spins in fully protonated samples.[5−9] More recently it has been demonstrated that fractional substitution of deuterons for protons bound to ^{13}C nuclei in combination with deuterium decoupling during periods where carbon magnetization evolves[10] can significantly decrease the rate of carbon relaxation.[11−13] This in turn results in an increase in the sensitivity and/or resolution of spectra that record carbon chemical shifts or in which carbon spins are involved in the relay of magnetization. Recent examples of the use of deuteration in concert with triple resonance spectroscopy include a 4D experiment which connects sequential amides in ^{15}N, ^{13}C, and ^{2}H labeled proteins[11] as well as constant time 3D HNCA (CT-HNCA) experiment.[13]

In this paper we describe a suite of triple resonance experiments for backbone assignments in ^{15}N, ^{13}C, ^{2}H labeled proteins. Included in this set of experiments are the CT-HNCA,[13] CT-HN(CO)CA, HN(CA)CB, HN(COCA)CB, and 4D HNCACB. The first pair of experiments link HN, ^{15}N, and $^{13}C^{\alpha}$ chemical shifts, while the second pair of experiments provide correlations connecting HN, ^{15}N, and $^{13}C^{\beta}$ shifts. The 4D HNCACB experiment links the HN and ^{15}N chemical shifts of a residue with intra- and inter-residue ($^{13}C^{\alpha}$, $^{13}C^{\beta}$) pairs. The experiments are very similar to non-deuterium versions published previously[3,4,14] but are designed to exploit the ^{13}C line narrowing effect that deuteration provides. The methods are demonstrated on a 37 kDa ternary complex of a ^{15}N, ^{13}C, 70% ^{2}H labeled sample of trp-repressor (trpR), fully protonated 5-methyltryptophan, and a fully protonated 20 basepair trp-operator DNA fragment. The signal-to-noise (S/N) of each experiment is evaluated, and the relative sensitivity differences

[†] Protein Engineering Centers of Excellence and Departments of Medical Genetics, Biochemistry, and Chemistry.

[‡] Ontario Cancer Institute and Department of Medical Biophysics.

[⊗] Abstract published in *Advance ACS Abstracts,* December 1, 1994.

(1) Bax, A.; Grzesiek, S. *Acc. Chem. Res.* **1993**, *26*, 131.
(2) Clore, G. M.; Gronenborn, A. *Science* **1991**, *252*, 1391.
(3) Ikura, M.; Kay, L. E.; Bax, A. *Biochemistry* **1990**, *29*, 4569.
(4) Kay, L. E.; Ikura, M.; Tschudin, R.; Bax, A. *J. Magn. Reson.* **1990**, *89*, 496.
(5) LeMaster, D. M.; Richards, F. M. *Biochemistry* **1988**, *27*, 142.
(6) Shon, K. J.; Opella, S. J. *Science* **1991**, *252*, 1303.
(7) Tsang, P.; Wright, P. E.; Rance, M. *J. Am. Chem. Soc.* **1990**, *112*, 8183.
(8) Arrowsmith, C. H.; Pachter, R.; Altman, R. B.; Iyer, S. B.; Jardetzky, O. *Biochemistry* **1990**, *29*, 6332.
(9) Reisman, J.; Hsu, V. L.; Parell, J.; Geiduschek, E. P.; Kearns, D. R. *J. Am. Chem. Soc.* **1991**, *113*, 2787.
(10) Browne, D. T.; Kenyon, G. L.; Packer, E. L.; Sternlicht, H.; Wilson, D. M. *J. Am. Chem. Soc.* **1973**, *95*, 1316.
(11) Gresiek, S.; Anglister, J.; Ren, H.; Bax, A. *J. Am. Chem. Soc.* **1993**, *115*, 4369.
(12) Kushlan, D. M.; LeMaster, D. M. *J. Biomol. NMR* **1993**, *3*, 701.
(13) Yamazaki, T.; Lee, W.; Revington, M.; Mattiello, D. L.; Dahlquist, F. W.; Arrowsmith, C. H.; Kay, L. E. *J. Am. Chem. Soc.* **1994**, *116*, 6464.
(14) Grzesiek, S.; Bax, A. *J. Magn. Reson.* **1992**, *96*, 432.

0002-7863/94/1516-11655$04.50/0

between recording spectra on a fully protonated vs a 70% deuterated sample are discussed. Finally, a comparison of the $^{13}C^{\alpha}$ T_2 values for ^{13}C spins one-bond coupled to either ^1H or ^2H is presented.

Experimental Section

Uniformly ^{15}N and ^{13}C labeled trpR was isolated from *E. coli* strain CY15070[15] containing the overproducing plasmid pJPR2 grown in 1−2 L of minimal media with $^{15}NH_4Cl$ and D-glucose-$^{13}C_6$ as the sole nitrogen and carbon sources, respectively. Purification was as described previously.[8,15] For triply labeled ^{15}N, ^{13}C, and ^2H trpR the cells were adapted to growth in D_2O as follows. Cells were first grown in M9 media with 200 μg/mL ampicillin and 33% D_2O as the solvent at 37 °C and then plated out onto an M9 agar plate made from 33% D_2O. A colony from the 33% plate was used to inoculate M9 media with 56% D_2O, cultured overnight at 37 °C, then plated onto a 56% D_2O M9 plate. For large-scale purification of triply labeled trpR, a single colony from the 56% plate was used to inoculate 10 mL of 70% D_2O M9 media containing $^{15}NH_4Cl$ and D-glucose-$^{13}C_6$. After overnight growth this culture was used to inoculate 1.5 L of the same M9 media. Although the cells grew a factor of 2 times more slowly than on normal M9 media, induction and purification yielded 60 mg of pure ^{15}N, ^{13}C, ^2H protein, similar to the amount normally obtained from H_2O growths. Protein−DNA complexes were prepared by adding the appropriate amount of synthetic operator DNA[16] to trpR followed by dialysis and concentration into a pH 6 solution of 50 mM sodium phosphate and a 4.8 mM racemic mixture of 5-methyltryptophan. Only the L-isomer has significant affinity for trpR.[17] Final NMR sample conditions were 2.4 mM trpR (trpR is a symmetric dimer of 108 amino acid monomers; 2.4 mM refers to the subunit concentration), 1.2 mM palindromic double stranded operator DNA, 2.4 mM 5-methyl-L-tryptophan, and 50 mM sodium phosphate adjusted to pH 6. The ^{15}N, ^{13}C fully protonated trpR sample used in the NMR studies was a factor of 2.6 lower in concentration relative to the ^{15}N, ^{13}C, ^2H sample.

All experiments were performed on a Varian UNITY 500 MHz spectrometer equipped with a pulsed field gradient unit and an actively shielded triple resonance probe head. Four separate synthesizers were used, one for the generation of each of ^1H, ^{13}C, ^{15}N, and ^2H pulses. The gating and modulation of rf from the ^{15}N and ^2H synthesizers were controlled by a single channel, requiring a number of small modifications to our spectrometer. On our spectrometer it was not possible to disable the ^2H lock receiver during either ^2H decoupling or the application of field gradient pulses; however, for improved spectrometer stability, the lock receiver should be gated off during ^2H decoupling or gradient pulses if possible. For the constant time HN(CO)CA(CT-HN(CO)CA) experiment, a matrix of 84* × 28* × 512* points (the * refers to complex points) was acquired with acquisition times of 25.7, 23.0, and 64.0 ms in each of t_1, t_2, and t_3. The corresponding spectral widths in F_1, F_2, and F_3 were 3268, 1217 and 8000 Hz. The total measuring time using eight scans per FID and a repetition delay of 2 s was 45 h. The HN(COCA)CB experiment was acquired as a 64* × 28* × 512* complex matrix with spectral widths of 9000, 1217, and 8000 Hz in F_1, F_2, and F_3 corresponding to acquisition times of 7.1, 23.0, and 64.0 ms in each of t_1, t_2, and t_3. A total of 16 scans were acquired per FID with a repetition delay of 1.8 s to give a total acquisition time of 62 h. The HN(CA)CB experiment was acquired as a 64* × 28* × 512* complex matrix with acquisition times of 8.3, 23.0, and 64.0 ms in each of t_1, t_2, and t_3. Spectral widths of 7650, 1217 and 8000 Hz in F_1, F_2, and F_3 were employed. A total of 16 scans were acquired per FID with a repetition delay of 1.8 s to give a total acquisition time of 62 h. The 4D HNCACB experiment was acquired as a 16* × 32* × 28* × 512* complex matrix with acquisition times of 7.1, 5.5, 23.0, and 64.0 ms in each of t_1, t_2, t_3, and t_4 and spectral widths of 2262, 5780, 1217, and 8000 Hz in F_1, F_2, F_3, and F_4. Two scans were acquired per FID with a repetition delay of 1.8 s to give a total acquisition time of 124 h. The CT-HNCA data set was acquired as described previously.[13]

All spectra were processed using nmrPipe/nmrDraw software developed by F. Delaglio, NIH,[18] and analyzed using the program PIPP.[19] In the acquisition dimension a solvent suppression filter was applied to the data to minimize the water signal[20] prior to apodization with a 65°-shifted squared sine-bell window function. The data were subsequently zero filled to twice the size and Fourier transformed. Only the downfield half of the spectrum was retained for the 3D data sets. In order to minimize space and processing time in the case of the 4D data set, only the HN region of the spectrum was retained in F_4 (7−10 ppm). In the case of the HN(CO)CA data set, the data were apodized in the $^{13}C^{\alpha}$ dimension using a 65°-shifted squared sine-bell window function, zero filled to 256 complex points followed by Fourier transformation, phasing, and elimination of the imaginary half of the signal. The size of the ^{15}N time domain was doubled via mirror image linear prediction,[21] apodized using a cosine-bell function, zero filled to 128 complex points, Fourier transformed, and phased, and imaginaries were eliminated. The absorptive part of the 3D data set was 256 × 128 × 512 real points. In principle, the $^{13}C^{\alpha}$ time domain could be extended via linear prediction as well, although this was not done in the present case. For the HN(COCA)CB and HN(CA)CB data sets, the data were apodized in the carbon dimension using a 65°-shifted squared sine-bell window function and zero filled to 128 complex points followed by Fourier transformation, phasing, and elimination of the imaginaries. In the case of the HN(COCA)CB spectrum a zero-order baseline correction was applied to the carbon dimension (after transformation and phasing) to correct for the dc offset introduced by the fact that the first point was not acquired at $t = 0$. The ^{15}N dimension was processed as described above to give a final absorptive data set of 128 × 128 × 512 points. For the 4D HNCACB spectrum the data were apodized in the $^{13}C^{\beta}$ dimension using a cosine-bell window function, zero filled to 64 complex data points, Fourier transformed, and phased and imaginaries discarded. In the ^{15}N dimension, after application of a cosine-bell window function, the data were zero filled to 64 complex data points, Fourier transformed, and phased and the imaginaries eliminated. Finally, the $^{13}C^{\alpha}$ time domain was extended to 32 points by mirror image linear prediction, apodized using a cosine-bell window function, zero filled to 64 complex data points, Fourier transformed, and phased and the imaginaries were discarded. The center of the $^{13}C^{\alpha}$ spectrum was shifted from 45 to 59 ppm by a frequency domain circular shift.[18] The final absorptive part of the data set consisted of 64 × 64 × 64 × 231 real points.

HN T_1 relaxation experiments were performed on the fully protonated sample using delays (T) of 0.1, 0.3, 0.5, 0.7, 1.5, 2.0, and 4.0 s. For the deuterated sample, delays of 0.2, 0.6, 1.0, 1.4, 2.0, 3.0, 4.0, and 8.0 s were employed. The $T_{1\rho}$ measurements were performed with the carbon carrier at 58 ppm using a 1.4 kHz spin lock field. Spin lock times of 4, 8, 12, 16, and 20 ms were used for the protonated sample, while times of 16, 32, 48, 80, 120, and 160 ms were employed for the deuterated sample.

Results and Discussion

The principal motivation for the substitution of ^2H for carbon-bound ^1H spins in ^{15}N and ^{13}C labeled proteins is the decrease in ^{13}C relaxation efficiency due to the approximately 7-fold lower gyromagnetic ratio of ^2H compared to ^1H.[10−13] Figure 1 shows the expected contributions to the carbon line width from both dipolar and chemical shift anisotropy (CSA) relaxation mechanisms for an isolated $^{13}C^{\alpha}-^1H^{\alpha}$ or $^{13}C^{\alpha}-^2H^{\alpha}$ spin pair as a function of isotropic molecular correlation time. Clearly the decrease in carbon line width as a result of the substitution of ^2H for ^1H is significant. For molecules with correlation times, τ_c, satisfying the relation $\tau_c \geq 10$ ns, the carbon line width is decreased by a factor of ~15 for a $^{13}C^{\alpha}$ one-bond coupled to a deuteron relative to a proton. The dramatic decrease in carbon relaxation rates with deuteration and the realization that a set

(15) Paluh, J. L.; Yanofsky, C. *Nucleic Acids Res.* **1986**, *14*, 7851.
(16) Lefevre, J. F.; Lane, A. N.; Jardetzky, O. *Biochemistry* **1987**, *26*, 5076.
(17) Marmostein, R. Q.; Joachimiak, A.; Sprinzl, M.; Sigler, P. B. *J. Biol. Chem.* **1987**, *262*, 4922.
(18) Delaglio, F. *nmrPipe System of Software*; National Institutes of Health: Bethesda, MD, 1993.
(19) Garrett, D. S.; Powers, R.; Gronenborn, A. M.; Clore, G. M. *J. Magn. Reson.* **1991**, *95*, 214.
(20) Marion, D.; Ikura, M.; Bax, A. *J. Magn. Reson.* **1989**, *84*, 425.
(21) Zhu, G.; Bax, A. *J. Magn. Reson.* **1990**, *90*, 405.

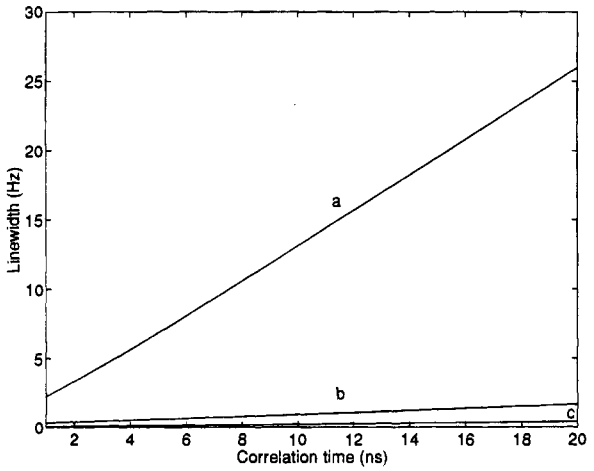

Figure 1. Expected contributions to the $^{13}C^{\alpha}$ line width from both dipolar and CSA relaxation assuming an isolated $^{13}C^{\alpha}$—$^{1}H^{\alpha}$ or $^{13}C^{\alpha}$—$^{2}H^{\alpha}$ spin pair attached to a molecule tumbling isotropically in solution. Curve a is the contribution to the line width from dipolar interactions with a directly attached ^{1}H at a distance of 1.10 Å;[42] curve b illustrates the dipolar contributions from a directly attached deuteron; curve c shows the contributions from CSA assuming an axially symmetric chemical shift tensor with $\Delta\sigma = 34$ ppm.[41]

of high-sensitivity experiments can be derived which exploits this result has led us to develop the suite of pulse schemes illustrated in Figure 2a–d for the backbone assignment of proteins that are ^{15}N, ^{13}C, ^{2}H labeled. An additional member of this family of experiments, the CT-HNCA, has been published previously.[13] Because all of the experiments make use of the "out and back" approach for magnetization transfer whereby magnetization both originates and is detected on the HN spin and since none of the transfer steps or evolution periods involve aliphatic/aromatic ^{1}H magnetization, these experiments will work most efficiency for samples with significant levels of deuterium enrichment. The temptation to prepare a fully deuterated sample is best resisted however since complete deuteration of a sample precludes its use for experiments which require that magnetization originate or be detected on carbon-bearing protons. In addition, full deuteration will likely result in a significant increase in HN T_1 relaxation times which would necessitate the use of longer relaxation delays. For this reason, it is unlikely that a fully deuterated sample will prove optimal for structural studies. We have therefore produced a 70% ^{2}H labeled trpR sample to be used in the present studies, and where necessary (see below), the experiments have been optimized for samples that are not fully labeled in deuterium.

Because the sequences are closely related to ^{15}N, ^{13}C triple resonance experiments that have been discussed in detail in the literature previously, we will not attempt to provide a quantitative explanation of each experiment here. Rather we highlight the unique features of these pulse sequences and provide a rationale for their design. Pulsed field gradients are employed in all of the experiments in order to minimize artifacts and the residual water in spectra[22–24] as well as to select for the coherence transfer pathway whereby magnetization passes through nitrogen in the final portion of each of the sequences.[25–27] An enhanced sensitivity approach is used to optimize signal-to-noise (S/N).[28,29] In addition, saturation/dephasing of water magnetization is kept to a minimum by ensuring that (i) homospoil gradient pulses are applied only when the water magnetization is stored along the z axis and that (ii) the water magnetization is placed along the $+z$ axis immediately prior to detection. In this context, each pulse scheme makes use of selective water pulses as described previously.[30–32]

The flow of magnetization transfer in each of the experiments can be described concisely by

$$\mathrm{HN} \xrightarrow{J_{\mathrm{HN}}} {}^{15}\mathrm{N} \xrightarrow{J_{\mathrm{NC}^{\alpha}}} {}^{13}\mathrm{C}^{\alpha}(t_1) \xrightarrow{J_{\mathrm{NC}^{\alpha}}} {}^{15}\mathrm{N}(t_2) \xrightarrow{J_{\mathrm{HN}}} \mathrm{HN}(t_3) \qquad \text{(3D CT-HNCA)}$$

$$\mathrm{HN} \xrightarrow{J_{\mathrm{HN}}} {}^{15}\mathrm{N} \xrightarrow{J_{\mathrm{NC'}}} {}^{13}\mathrm{CO}_{(i-1)} \xrightarrow{J_{\mathrm{C'C}^{\alpha}}} {}^{13}\mathrm{C}^{\alpha}_{(i-1)}(t_1) \xrightarrow{J_{\mathrm{C'C}^{\alpha}}} {}^{13}\mathrm{CO}_{(i-1)} \xrightarrow{J_{\mathrm{NC'}}} {}^{15}\mathrm{N}(t_2) \xrightarrow{J_{\mathrm{HN}}} \mathrm{HN}(t_3) \qquad \text{(3D CT-HN(CO)CA)}$$

$$\mathrm{HN} \xrightarrow{J_{\mathrm{HN}}} {}^{15}\mathrm{N} \xrightarrow{J_{\mathrm{NC'}}} {}^{13}\mathrm{CO}_{(i-1)} \xrightarrow{J_{\mathrm{C'C}^{\alpha}}} {}^{13}\mathrm{C}^{\alpha}_{(i-1)} \xrightarrow{J_{\mathrm{CC}}} {}^{13}\mathrm{C}^{\beta}_{(i-1)}(t_1) \xrightarrow{J_{\mathrm{CC}}} {}^{13}\mathrm{C}^{\alpha}_{(i-1)} \xrightarrow{J_{\mathrm{C'C}^{\alpha}}} {}^{13}\mathrm{CO}_{(i-1)} \xrightarrow{J_{\mathrm{NC'}}} {}^{15}\mathrm{N}(t_2) \xrightarrow{J_{\mathrm{HN}}} \mathrm{HN}(t_3) \qquad \text{(3D HN(COCA)CB)}$$

$$\mathrm{HN} \xrightarrow{J_{\mathrm{HN}}} {}^{15}\mathrm{N} \xrightarrow{J_{\mathrm{NC}^{\alpha}}} {}^{13}\mathrm{C}^{\alpha} \xrightarrow{J_{\mathrm{CC}}} {}^{13}\mathrm{C}^{\beta}(t_1) \xrightarrow{J_{\mathrm{CC}}} {}^{13}\mathrm{C}^{\alpha} \xrightarrow{J_{\mathrm{NC}^{\alpha}}} {}^{15}\mathrm{N}(t_2) \xrightarrow{J_{\mathrm{HN}}} \mathrm{HN}(t_3) \qquad \text{(3D HN(CA)CB)}$$

$$\mathrm{HN} \xrightarrow{J_{\mathrm{HN}}} {}^{15}\mathrm{N} \xrightarrow{J_{\mathrm{NC}^{\alpha}}} {}^{13}\mathrm{C}^{\alpha}(t_1) \xrightarrow{J_{\mathrm{CC}}} {}^{13}\mathrm{C}^{\beta}(t_2) \xrightarrow{J_{\mathrm{CC}}} {}^{13}\mathrm{C}^{\alpha} \xrightarrow{J_{\mathrm{NC}^{\alpha}}} {}^{15}\mathrm{N}(t_3) \xrightarrow{J_{\mathrm{HN}}} \mathrm{HN}(t_4) \qquad \text{(4D HNCACB)}$$

For completeness, the transfer path in the CT-HNCA experiment[13] is provided as well. The relevant couplings involved in each of the magnetization transfer steps are indicated above the arrows, and t_1, t_2, t_3, and t_4 denote acquisition times.

The CT-HNCA and CT-HN(CO)CA experiments provide correlations of the form ($^{13}C^{\alpha}$, ^{15}N, HN) with the $^{13}C^{\alpha}$ and ^{15}N chemical shifts recorded in a constant time manner.[33–34] Note that the HNCA experiment provides both intra- and inter-residue correlations, while the HN(CO)CA provides only sequential connectivities. In both of the CT-HNCA and CT-HN(CO)CA experiments, ^{13}C magnetization is recorded during a delay which is set to $1/(J_{CC})$, where J_{CC} is the one-bond aliphatic carbon–carbon scalar coupling. The increased acquisition time in the carbon dimension (~27 ms) relative to previous versions of these experiments[3,4,14] (~8 ms) coupled with the fact that the significant one-bond homonuclear $^{13}C^{\alpha}$—$^{13}C^{\beta}$ coupling does not modulate the time domain carbon signal in the constant time experiments results in over three times the resolution in this dimension. The choice of a constant time delay of $1/(J_{CC}) \sim$ 27 ms ensures that the majority of correlations in spectra of

(22) Hurd, R. E.; John, B. K. *J. Magn. Reson.* **1991**, *91*, 648.
(23) Von Kienlin, M.; Moonen, C. T. W.; Van Der Toorn, A.; Van Zijl, P. C. M. *J. Magn. Reson.* **1991**, *93*, 423.
(24) Bax, A.; Pochapsky, S. *J. Magn. Reson.* **1992**, *99*, 638.
(25) Kay, L. E.; Keiffer, P.; Saarien, T. *J. Am. Chem. Soc.* **1992**, *114*, 10663.
(26) Schleucher, J.; Sattler, M.; Griesinger, C. *Angew. Chem., Int. Ed. Engl.* **1993**, *10*, 32.
(27) Muhandiram, D. R.; Kay, L. E. *J. Magn. Reson. B* **1994**, *103*, 203.
(28) Cavanagh, J.; Palmer, A. G.; Wright, P. E.; Rance, M. *J. Magn. Reson.* **1991**, *91*, 429.
(29) Palmer, A. G.; Cavanagh, J.; Wright, P. E.; Rance, M. *J. Magn. Reson.* **1991**, *93*, 151.
(30) Grzesiek, S.; Bax, A. *J. Am. Chem. Soc.* **1993**, *115*, 12593.
(31) Stonehouse, J.; Shaw, G. L.; Keeler, J.; Laue, E. *J. Magn. Reson. A* **1994**, *107*, 178.
(32) Kay, L. E.; Xu, G. Y.; Yamazaki, T. *J. Magn. Reson. A* **1994**, *109*, 129.
(33) Santoro, J.; King, G. C. *J. Magn. Reson.* **1992**, *97*, 202.
(34) Vuister, G. W.; Bax, A. *J. Magn. Reson.* **1993**, *101*, 201.

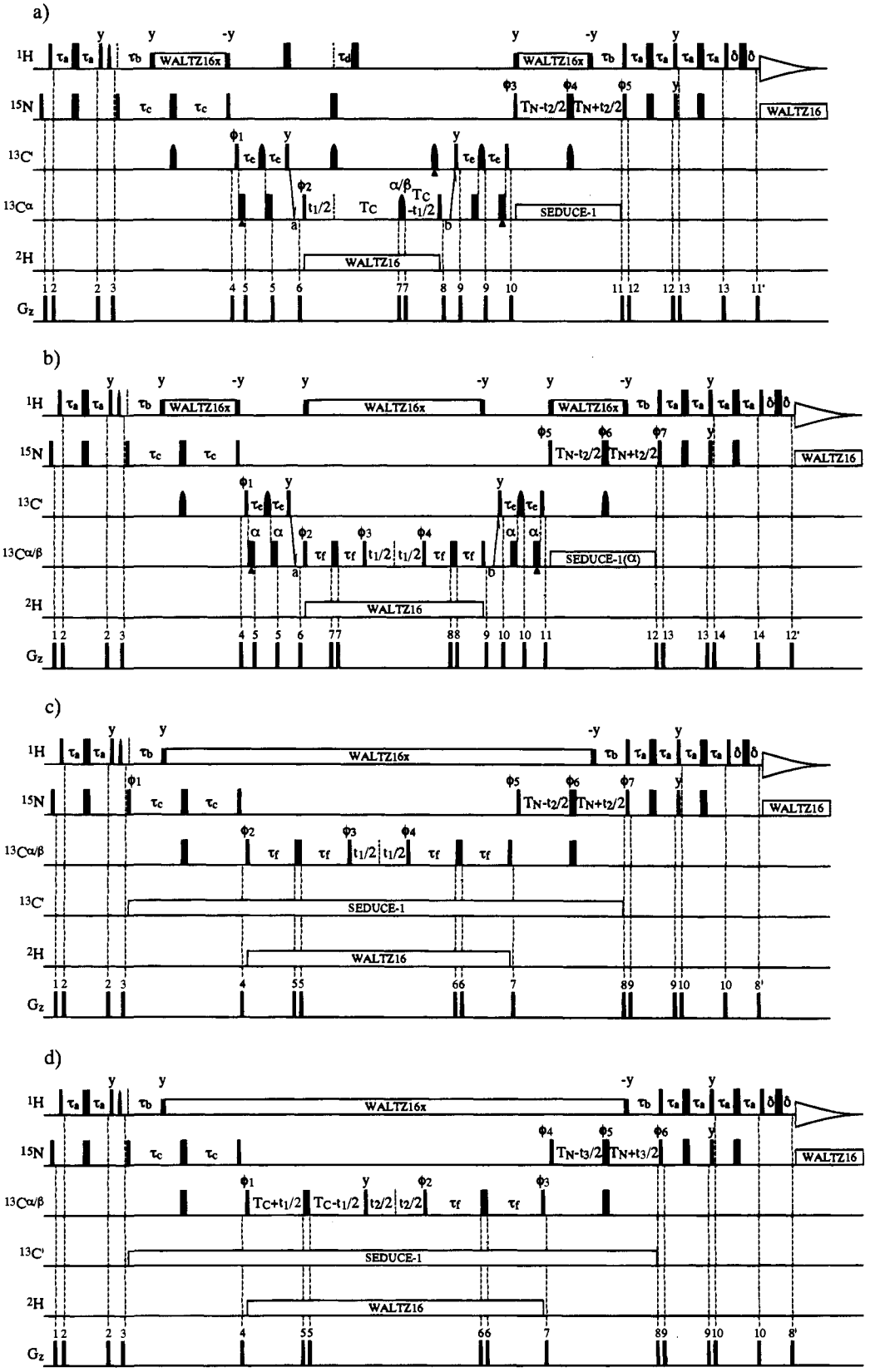

Figure 2. Pulse schemes of the (a) 3D CT-HN(CO)CA, (b) 3D HN(COCA)CB, (c) 3D HN(CA)CB, and (d) 4D HNCACB experiments. All narrow (wide) pulses are applied with a flip angle of 90° (180°). Unless indicated otherwise, pulses are applied along the x axis. The ^{1}H and ^{15}N carriers are centered at 4.7 ppm (water) and 119 ppm, respectively. Proton pulses are applied using a 23 kHz field with the exception of the water selective 90° pulse during the first INEPT transfer[43] (indicated by the shaped ^{1}H pulse in the sequences) which is applied either as a 2 ms rectangular pulse or as a 2 ms pulse with the SEDUCE-1[44] profile, the 6.8 kHz $\pm y$ pulses flanking the WALTZ-16$_x$[45] decoupling periods and the 6.8 kHz WALTZ-16$_x$[45] decoupling sequence. (Note that in WALTZ-16$_x$ all of the rf pulses are of phase x or $-x$.) The ^{15}N pulses are applied using a 5.2 kHz field, with ^{15}N decoupling during acquisition using a 1 kHz field. All carbon pulses were applied using only a single frequency source. *All decoupling is interrupted during the application of the gradient pulses.*[46] *In the case of ^{1}H decoupling, the water magnetization must first be "returned" to the z axis prior to application of the gradient pulse and subsequently rotated to the decoupling axis prior to the continuation of*

Figure 2 caption continued

decoupling.[32] Sequence a, CT-HN(CO)CA: Carbonyl 180° pulses are applied using the SEDUCE-1[44] profile with a peak amplitude of 4.72 kHz corresponding to a length of 230 μs. The pulses are centered at 176 ppm. At point a in the sequence the carbon carrier is jumped from 176 to 58 ppm and subsequently returned to 176 ppm at point b. Therefore the $^{13}C'$ 180° pulses between points a and b are applied as phase modulated pulses.[47,48] The $^{13}C'$ and $^{13}C^{\alpha}$ 90° pulses are applied using a field strength of 3.93 kHz so that application of $^{13}C'$ pulses minimizes excitation of $^{13}C^{\alpha}$ spins and vice versa.[4] All $^{13}C^{\alpha}$ 180° pulses (8.78 kHz) with the exception of the 180° pulse during the $2T_C$ period (400 μs RE-BURP[49] pulse with a peak amplitude of 15.7 kHz, affecting both $^{13}C^{\alpha}$ and $^{13}C^{\beta}$ spins) are applied as phase-modulated rectangular pulses since the carbon carrier is centered at 176 ppm during application of these pulses. The positions of the Bloch–Siegert compensation pulses[34] are indicated by the arrowheads in the figure. $^{13}C^{\alpha}$ decoupling is achieved using a 118 ppm cosine-modulated WALTZ-16[45] field employing pulses having the SEDUCE-1[50] profile (330 μs 90° pulses). ^{2}H decoupling is achieved using a 0.9 kHz WALTZ-16[45] sequence centered at 4.5 ppm. The delays employed are $\tau_a = 2.3$ ms, $\tau_b = 5.5$ ms, $\tau_c = 12$ ms, $\tau_d = 1.7$ ms, $\tau_e = 4.1$ ms, $T_C = 13.8$ ms, $T_N = 12$ ms, $\delta = 0.5$ ms. The phase cycling employed is $\phi_1 = (x, -x)$; $\phi_2 = 2(x),2(-x)$; $\phi_3 = x$; $\phi_4 = 4(x),4(-x)$; $\phi_5 = x$; rec = $(x,-x,-x,x)$. Quadrature in F_1 is achieved via States-TPPI[51] of ϕ_2. For each value of t_2, N- and P-type coherences are obtained by recording two data sets whereby the sign of the gradient g_{11} is inverted and 180° added to the phase of ϕ_5 for the second data set. Data sets obtained in an interleaved manner for positive and negative g_{11} values are stored in separate memory locations and pure absorptive line shapes in the ^{15}N dimension generated by adding and subtracting the N- and P-type data sets, storing the new data sets separately and applying a 90° zero-order phase correction in the acquisition dimension to one (not both) of the new data sets.[25] The phase of ϕ_3 and the phase of the receiver are incremented by 180° for each increment of t_2.[51] The durations and strengths of the gradients (rectangular) are g_1 = (0.5 ms, 8 G/cm), g_2 = (0.5 ms, 4 G/cm), g_3 = (1.0 ms, 10 G/cm), g_4 = (1.0 ms, 1 G/cm), g_5 = (1.0 ms, 7 G/cm), g_6 = (1 ms, −15 G/cm), g_7 = (0.2 ms, 20 G/cm), g_8 = (1 ms, 8 G/cm), g_9 = (1 ms, 0.4 G/cm), g_{10} = (0.6 ms, 10 G/cm), g_{11} = (1.25 ms, 30 G/cm), $g_{11'}$ = (0.125 ms, 27.8 G/cm), g_{12} = (0.5 ms, 8 G/cm), g_{13} = (0.3 ms, 2 G/cm). Note that the effect of all of the ^{1}H pulses on water is such that the water magnetization is restored to the $+z$ axis at the start of acquisition. Sequence b, HN(COCA)CB: Many of the details of this sequence are similar to those of sequence a. Only the differences are described here. At point a in the sequence the carbon carrier is jumped from 176 to 43 ppm and subsequently returned to 176 ppm at point b. The $^{13}C^{\alpha/\beta}$ pulses marked α (8.78 kHz field) are applied as phase-modulated pulses so that the center of the excitation is at 58 ppm. Additionally, $^{13}C^{\alpha}$ decoupling is achieved using a 118 ppm cosine-modulated WALTZ-16[45] field employing pulses having the SEDUCE-1[50] profile as before (i.e., the center of the decoupling field is at 58 and not 43 ppm). All other $^{13}C^{\alpha/\beta}$ pulses are applied so that the excitation is centered at 43 ppm. The $^{13}C^{\alpha/\beta}$ 90° pulses are applied using a 4.25 kHz field, while the 180° pulses are applied with a 9.51 kHz field to minimize excitation of carbonyl magnetization.[4] Since $^{13}C^{\beta}$ (not $^{13}C^{\alpha}$) chemical shifts of all the amino acids with the exception of glycine are recorded during t_1, it is not necessary to apply an ^{15}N 180° pulse in the center of the t_1 evolution period. If a smaller value of τ_f is employed to obtain both $^{13}C^{\alpha}$ and $^{13}C^{\beta}$ shifts or for (very) slightly better sensitivity of glycine cross peaks, a 180° ^{15}N pulse can be applied in the middle of the t_1 period for those values of t_1 satisfying the relation $t_1 > \tau_{180}$, where τ_{180} is the ^{15}N 180° pulse width. For $t_1 < \tau_{180}$, the ^{15}N 180° pulse is applied immediately after the $^{13}C^{\alpha/\beta}$ pulse of phase ϕ_4. The application of the ^{15}N 180° pulse in this manner minimizes baseline distortions in the carbon dimension caused by a nonideal initial t_1 value. It is possible to insert a C' 180° pulse in the center of the t_1 period to improve (slightly) the sensitivity of correlations involving glycine or asparagine/aspartic acid residues; however, because of the length of such a pulse, it is necessary to back-predict the first couple of points in this dimension. The delay τ_f is set to 6.8 ms. The phase cycling employed is $\phi_1 = (x,-x)$; $\phi_2 = 2(x),2(-x)$; $\phi_3 = 4(y),4(-y)$; $\phi_4 = 8(y),8(-y)$; $\phi_5 = x$; $\phi_6 = 4(x),4(-x)$; $\phi_7 = x$; rec = $(x,-x,-x,x)$. Quadrature in F_1 is achieved via States-TPPI[51] of ϕ_2 and ϕ_3. For each value of t_2, N- and P-type coherences are obtained by recording two data sets whereby the sign of the gradient g_{12} is inverted and 180° added to the phase ϕ_7 for the second data set.[25] In addition the phase ϕ_5 and the phase of the receiver are incremented by 180° for each new value of t_2.[51] The durations and strengths of the gradients (rectangular) are g_1 = (0.5 ms, 8 G/cm), g_2 = (0.5 ms, 4 G/cm), g_3 = (1.0 ms, 10 G/cm), g_4 = (1.0 ms, 1 G/cm), g_5 = (1.0 ms, 7 G/cm), g_6 = (1 ms, 15 G/cm), g_7 = (1 ms, 1 G/cm), g_8 = (0.5 ms, 10 G/cm), g_9 = (1 ms, 8 G/cm), g_{10} = (1 ms, 0.4 G/cm), g_{11} = (0.6 ms, 10 G/cm), g_{12} = (1.25 ms, 30 G/cm), $g_{12'}$ = (0.125 ms, 27.8 G/cm), g_{13} = (0.5 ms, 8 G/cm), g_{14} = (0.3 ms, 2 G/cm). Sequence c, HN(CA)CB: All $^{13}C^{\alpha/\beta}$ pulses are applied with the ^{13}C carrier centered at 43 ppm using an 18 kHz field. $^{13}C'$ decoupling is achieved using a 133 ppm cosine-modulated WALTZ-16[45] field employing pulses having the SEDUCE-1[50] profile (i.e., the carbon carrier is at 43 ppm). The delays used are as given above. For (very) slightly better sensitivity for glycine residues or if a shorter τ_f value is employed, a 180° ^{15}N pulse can be inserted in the center of the t_1 period as described for the HN(COCA)CB experiment. The phase cycling employed is $\phi_1 = (x,-x)$; $\phi_2 = 2(x),2(-x)$; $\phi_3 = 4(y),4(-y)$; $\phi_4 = 8(y),8(-y)$; $\phi_5 = x$; $\phi_6 = 4(x),4(-x)$; $\phi_7 = x$; rec = $(x,-x,-x,x)$. Quadrature in F_1 is achieved via States-TPPI[51] of ϕ_2 and ϕ_3. Quadrature in F_2 is achieved using the gradient approach described above with the phase ϕ_7 and the sign of the gradient g_8 inverted to generate N- and P-type data sets.[25] The phase ϕ_5 and the phase of the receiver are incremented by 180° for each new value of t_2.[51] The durations and strengths of the gradients (rectangular) are g_1 = (0.5 ms, 8 G/cm), g_2 = (0.5 ms, 4 G/cm), g_3 = (1.0 ms, 10 G/cm), g_4 = (0.5 ms, 8 G/cm), g_5 = (0.1 ms, 20 G/cm), g_6 = (0.1 ms, 30 G/cm), g_7 = (0.6 ms, 10 G/cm), g_8 = (1.25 ms, 30 G/cm), $g_{8'}$ = (0.125 ms, 27.8 G/cm), g_9 = (0.5 ms, 8 G/cm), g_{10} = (0.3 ms, 2 G/cm). Sequence d, 4D HNCACB: Almost all details are the same as those for HN(CA)CB. The carbon carrier is centered at 45 ppm and $^{13}C'$ decoupling achieved using a 131 ppm cosine-modulated WALTZ-16[45] field employing pulses having the SEDUCE-1[50] profile. The value of T_C is set to 6.8 ms. The phase cycling employed is $\phi_1 = (x,-x)$; $\phi_2 = y$; $\phi_3 = x$; $\phi_4 = x$; $\phi_5 = (x,-x)$; $\phi_6 = x$; rec = $(x,-x)$. Quadrature in F_1 is achieved via States-TPPI[51] of ϕ_1. Quadrature in F_2 is achieved via States-TPPI of ϕ_2 and ϕ_3. Quadrature in F_3 is achieved using the gradient approach described above with the phase ϕ_6 and the sign of the gradient g_8 inverted to generate N- and P-type data sets.[25] The phase ϕ_4 and the phase of the receiver are incremented by 180° for each new value of t_3.[51] The durations and strengths of the gradients are as described for the HN(CA)CB sequence.

proteins that are fractionally deuterated arise from ^{13}C spins that are one-bond coupled to deuterons and not protons. Assuming isotropic molecular tumbling with a correlation time of 15 ns (MW ~30 000) and including only the contribution to the relaxation of the $^{13}C^{\alpha}$ spin from dipolar interactions with the directly attached ^{1}H or ^{2}H spin, $^{13}C^{\alpha}$ T_2 values of 16 ms ($^{13}C-^{1}H$) and 249 ms ($^{13}C-^{2}H$) are calculated. Thus, during a constant time period of $1/(J_{CC})$, the intensities of cross peaks arising from $^{13}C^{\alpha}-^{2}H$ as opposed to $^{13}C^{\alpha}-^{1}H$ pairs are roughly in the ratio of 5 to 1, assuming 50% fractional deuteration at the C^{α} position. For those residues displaying increased mobility and subsequently increased $^{13}C^{\alpha}$ T_2 values, it is very likely that cross peaks of significant intensity will arise from $^{13}C^{\alpha}$ spins coupled to either ^{1}H or ^{2}H. Because of the significant one-bond deuterium isotope shift of approximately 0.4 ppm,[11-13] the doubling of signals degrades spectral resolution in the carbon dimension. In order to avoid this problem in the CT-HN(CO)-CA scheme of Figure 2a, we have made use of an approach described previously[13] whereby carbon magnetization arising from $^{13}C^{\alpha}-^{1}H^{\alpha}$ pairs evolves during the constant time period $2T_C$ for a duration $2\tau_d = 1/(2J_{HC})$. In this way this magnetization is antiphase immediately after the $2T_C$ period and is not refocused into an observable signal by the remaining pulses.

Figure 2, parts b and c, illustrate the HN(COCA)CB and HN-(CA)CB pulse sequences, respectively. The HNCACB experiment was originally developed by Wittekind and Mueller[35] based on the CBCANH scheme of Grzesiek and Bax[36] and provides correlations of the form ($^{13}C^{\alpha}/^{13}C^{\beta}$, ^{15}N, HN). As in the HNCA experiment, correlations of both the intra- and the inter-residue variety can be obtained from this experiment. In contrast the

HN(COCA)CB experiment provides correlations linking sequential shifts exclusively. Note that cross peaks linking either the $^{13}C^{\alpha}$ or $^{13}C^{\beta}$ shifts are proportional in intensity to $\cos^2(2\pi J_{CC}\tau_f)$ or $\sin^2(2\pi J_{CC}\tau_f)$, respectively. Therefore by tuning the value of τ_f suitably it is possible to select for either $^{13}C^{\alpha}$ or $^{13}C^{\beta}$ cross peaks. For ^{15}N, ^{13}C labeled samples, Wittekind and Mueller[35] and Grzesiek and Bax[36] have chosen $\tau_f \sim 1/(8J_{CC})$ so that both sets of peaks are obtained, albeit at half of the maximum intensity possible neglecting relaxation losses and pulse imperfections. Because of the rapid $^{13}C^{\alpha}$ relaxation that occurs in fully protonated samples, it is not practical to choose $\tau_f \sim 1/(4J_{CC})$ to optimize transfer to the $^{13}C^{\beta}$ carbon in any event. In contrast, for studies with the ^{15}N, ^{13}C, 70% ^{2}H sample of trpR described here, we prefer to obtain ($^{13}C^{\alpha}$, ^{15}N, HN) correlations from the CT-HNCA/CT-HN(CO)CA experiments described above and ($^{13}C^{\beta}$, ^{15}N, HN) correlations from HN(CA)CB/HN(COCA)CB experiments optimized for transfer of magnetization from $^{13}C^{\alpha}$ to $^{13}C^{\beta}$ $\{\tau_f \sim 1/(4J_{CC})\}$. For this reason we have referred to these experiments as HN(CA)CB and HN(COCA)CB in keeping with the nomenclature introduced by Ikura *et al.*[3] Neglecting relaxation and pulse imperfections, the sensitivities of the ($^{13}C^{\beta}$, ^{15}N, HN) peaks in the HNCACB experiment with $\tau_f \sim 1/(8J_{CC})$ are reduced by a factor of 2 relative to cross peaks recorded in the HN(CA)CB experiment. In a similar vein, ($^{13}C^{\alpha}$, ^{15}N, HN) cross peaks in the HNCACB experiment recorded with $\tau_f \sim 1/(8J_{CC})$ are a factor of 2 reduced in intensity relative to the corresponding peaks obtained from an HNCA experiment recorded in exactly the same manner. Thus for equal S/N the HNCACB experiment which provides both $^{13}C^{\alpha}$ and $^{13}C^{\beta}$ correlations $\{\tau_f \sim 1/(8J_{CC})\}$ must be recorded for a period which is twice as long as the *combined* measuring times of the HNCA and HN(CA)CB $\{\tau_f \sim 1/(4J_{CC})\}$ experiments. Similar conclusions hold for the HN(CO)CACB experiment $\{\tau_f \sim 1/(8J_{CC})\}$ vs the HN(COCA)CB $\{\tau_f \sim 1/(4J_{CC})\}$ and HN(CO)CA experiments. As will be illustrated later, for proteins with significant levels of deuterium enrichment (such as the 70% ^{2}H sample considered in the present study), higher quality spectra are obtained by recording pairs of experiments which optimize a specific magnetization transfer rather than recording a single spectrum where the sensitivity of all correlations is compromised.

As has been described above, the HNCA and HN(CO)CA experiments are recorded with constant time in the carbon dimension. This is particularly important given the (often) poor dispersion in the $^{13}C^{\alpha}$ dimension of protein spectra. In contrast, we have found that for the level of enrichment of ^{2}H in the trpR sample that we are studying (~70%) experiments which measure the $^{13}C^{\beta}$ chemical shift using a similar constant time strategy suffer significantly from sensitivity losses relative to their nonconstant time counterparts. Note that, in the HN(CA)CB/HN(COCA)CB experiments, cross peaks providing the $^{13}C^{\beta}$ chemical shift arise from magnetization that is transferred from $^{13}C^{\alpha}$ to $^{13}C^{\beta}$. The process of completely transferring magnetization from $^{13}C^{\alpha}$ to $^{13}C^{\beta}$ and then back (after $^{13}C^{\beta}$ t_1 evolution) dictates that the magnetization resides on the $^{13}C^{\alpha}$ spin in the transverse plane for ~27 ms. In the case of constant time carbon evolution, magnetization residues further on the β-carbon for ~27 ms ($1/J_{CC}$). For high sensitivity it is crucial that all carbons involved in the magnetization transfer process (in this case $^{13}C^{\alpha}$ and $^{13}C^{\beta}$) be fully deuterated. In the case of ~70% deuteration, only ~35% of the population of molecules satisfy this constraint, assuming random deuteration, and the subsequent degradation of sensitivity unfortunately precludes the use of constant time carbon evolution. Since a large fraction of the signal comes from $^{13}C^{\beta}$ spins that are coupled to protons in this case, it is necessary to employ ^{1}H decoupling during the recording of carbon magnetization in the HN(CA)CB or HN(COCA)CB experiments. Recall that in the case of experiments which record only $^{13}C^{\alpha}$ chemical shift in a constant time manner ^{1}H decoupling is not necessary during the constant time evolution since the majority of the detected signal originates from carbons that are one-bond coupled to ^{2}H and not ^{1}H. Moreover, a purging scheme is employed which selects for the $^{13}C^{\alpha}-^{2}H^{\alpha}$ population of molecules.[13] Clearly such a purging scheme should not be employed in the case of the HN(CA)CB or HN(COCA)CB experiments. In any event, the significantly lower resolution in the carbon dimension in the $^{13}C^{\beta}$ experiments due to the coarse digitization used obviates the need to employ a purging scheme to eliminate the extra peaks caused by the deuterium isotope shift.

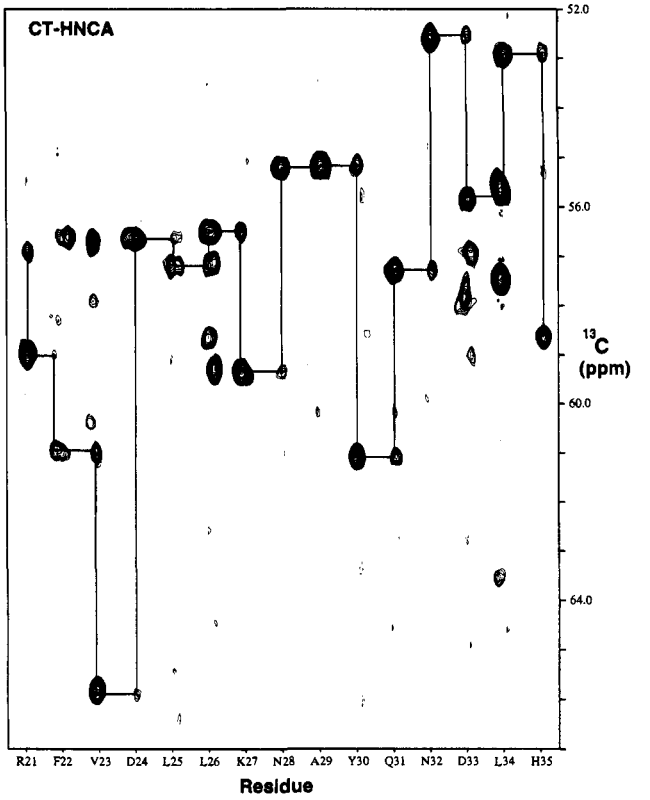

Figure 3. Strip plot showing the region of the CT-HNCA spectrum of trpR complex from R21 to H35. Both intra- and inter-residue correlations are available from this experiment. The sequential connectivity derived from the analysis of the experiments presented is indicated here and in Figures 4–6 by lines connecting the appropriate intra-/inter-residue cross peaks.

Figures 3–6 demonstrate the applications of the various 3D pulse schemes to the ternary complex of trpR, 5-methyltryptophan, and a 20 basepair trp-operator DNA sequence (MW 37 000). In particular, strip plots comprising residues R21–H35 are illustrated, taken at the ^{15}N and HN frequencies of the residues indicated. Clearly the sensitivity afforded by these experiments is excellent. In the figures illustrating the HN(COCA)CB and HN(CA)CB experiments (Figures 5 and 6, respectively), a portion of the $^{13}C^{\alpha}$ chemical shift region has been included to indicate that it is possible to achieve essentially complete transfer of magnetization from $^{13}C^{\alpha}$ to $^{13}C^{\beta}$ and therefore record only $^{13}C^{\beta}$ chemical shifts in these experiments through the judicious choice of τ_f (~7 ms). Note that signals from glycine residues are still present, albeit of opposite sign relative to other cross peaks.

A comparison of HNCACB spectra recorded with τ_f values of 3.5 ms (a) and 6.8 ms (b) (same measuring time for both spectra) is presented in Figure 7, where planes at an ^{15}N

(35) Wittekind, M.; Mueller, L. *J. Magn. Reson. B* **1993**, *101*, 201.
(36) Grzesiek, S.; Bax, A. *J. Magn. Reson.* **1992**, *99*, 201.

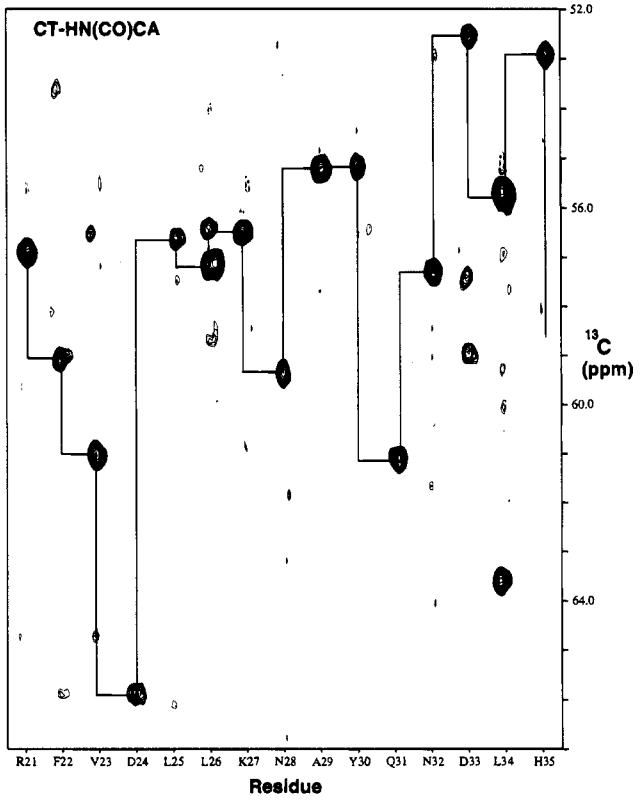

Figure 4. Strip plot of the CT-HN(CO)CA spectrum from R21 to H35. Only correlations connecting the ^{15}N and HN chemical shifts with the $^{13}C^{\alpha}$ shift of the preceding residue are obtained from this data set.

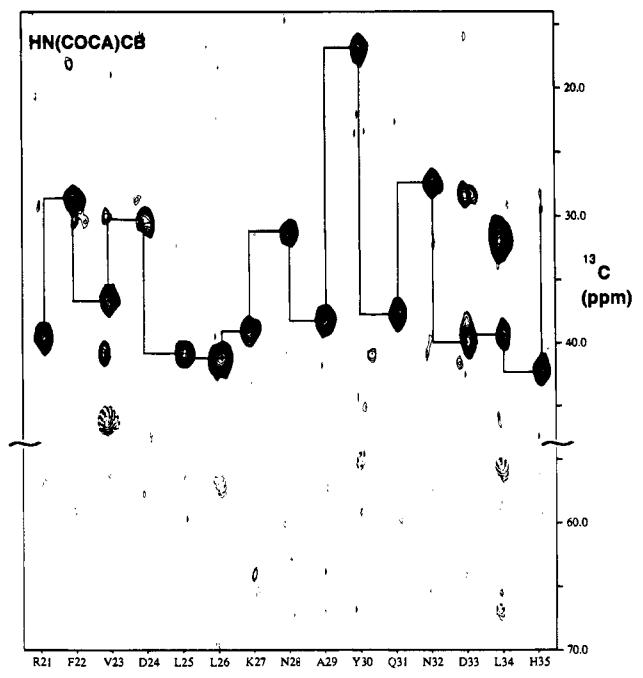

Figure 5. Strip plot of the HN(COCA)CB spectrum correlating $^{13}C^{\beta}$ $(i-1)$, ^{15}N (i), and HN (i) chemical shifts of R21–H35. $^{13}C^{\alpha}$ $(i-1)$, ^{15}N (i), and HN (i) correlations for glycine residues are also present in the spectrum, with opposite sign relative to the other peaks. The region from ~50 to ~70 ppm is illustrated to show that it is possible to efficiently suppress $^{13}C^{\alpha}$ $(i-1)$, ^{15}N (i), and HN (i) correlations of all residues with the exception of glycine by the suitable choice of delays in the HN(COCA)CB pulse scheme.

chemical shift of 116 ppm from each experiment are shown. Recall that a τ_f value of ~7 ms ensures virtually complete transfer from $^{13}C^{\alpha}$ to $^{13}C^{\beta}$ carbons in the scheme of Figure 2c

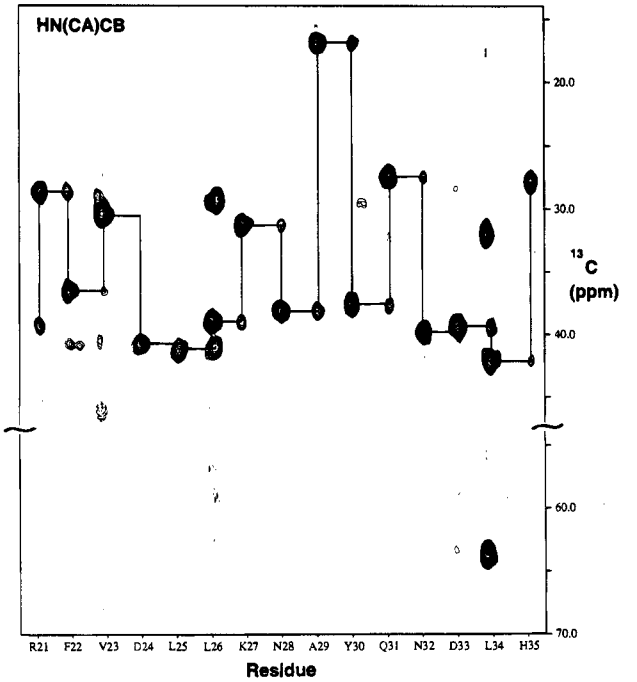

Figure 6. Strip plot of the HN(CA)CB spectrum correlating $^{13}C^{\beta}$ (i)/ $^{13}C^{\beta}$ $(i-1)$, ^{15}N (i), and HN (i) chemical shifts of residues R21–H35. As in the HN(COCA)CB spectrum, cross peaks of opposite sign are observed for glycine residues. The cross peak at a $^{13}C^{\beta}$ shift of 63.8 ppm is assigned to S107.

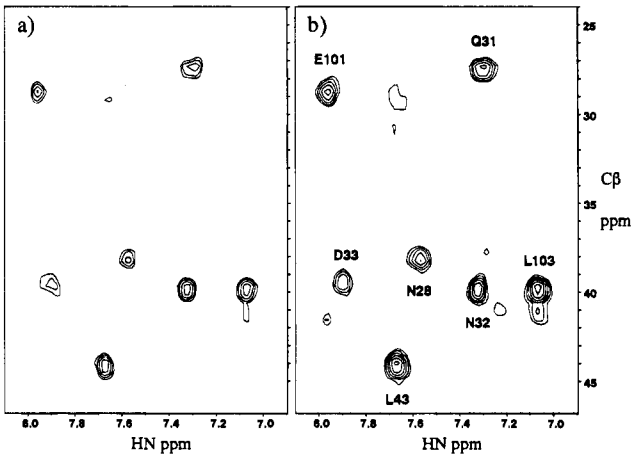

Figure 7. Comparison of HNCACB spectra recorded with τ_f values of 3.5 ms (a) and 6.8 ms (b). Equal measuring times were used for both spectra. A slice from each spectrum is presented at an ^{15}N chemical shift of 116 ppm. Contour levels are spaced a factor of $2^{1/2}$ apart in intensity. Only eight time points were recorded in the ^{15}N dimension for each of the 3D experiments in this case.

so that only ($^{13}C^{\beta}$, ^{15}N, HN) correlations are obtained while τ_f = 3.5 ms provides correlations to both $^{13}C^{\alpha}$ and $^{13}C^{\beta}$ spins. An approximate factor of 2 increase in sensitivity of ($^{13}C^{\beta}$, ^{15}N, HN) cross peaks (contours are spaced a factor of $2^{1/2}$ in intensity apart) in the spectrum recorded with the longer τ_f value is noted. For this reason and because of the excellent sensitivity and spectral resolution provided by the CT-HNCA/CT-HN(CO)-CA schemes (Figures 3 and 4), separate experiments have been recorded to obtain $^{13}C^{\alpha}$ and $^{13}C^{\beta}$ correlations.

Although the molecular mass of the trpR complex is 37 kDa, the protein portion of the complex is made up of a symmetric dimer with each monomer consisting of only 108 amino acids. Despite the predominantly α-helical nature of the molecule, the resolution afforded by the 3D methods described above is sufficient for the assignment of the $^{13}C^{\alpha}$, $^{13}C^{\beta}$, ^{15}N, and HN chemical shifts. However, for applications to single chain large

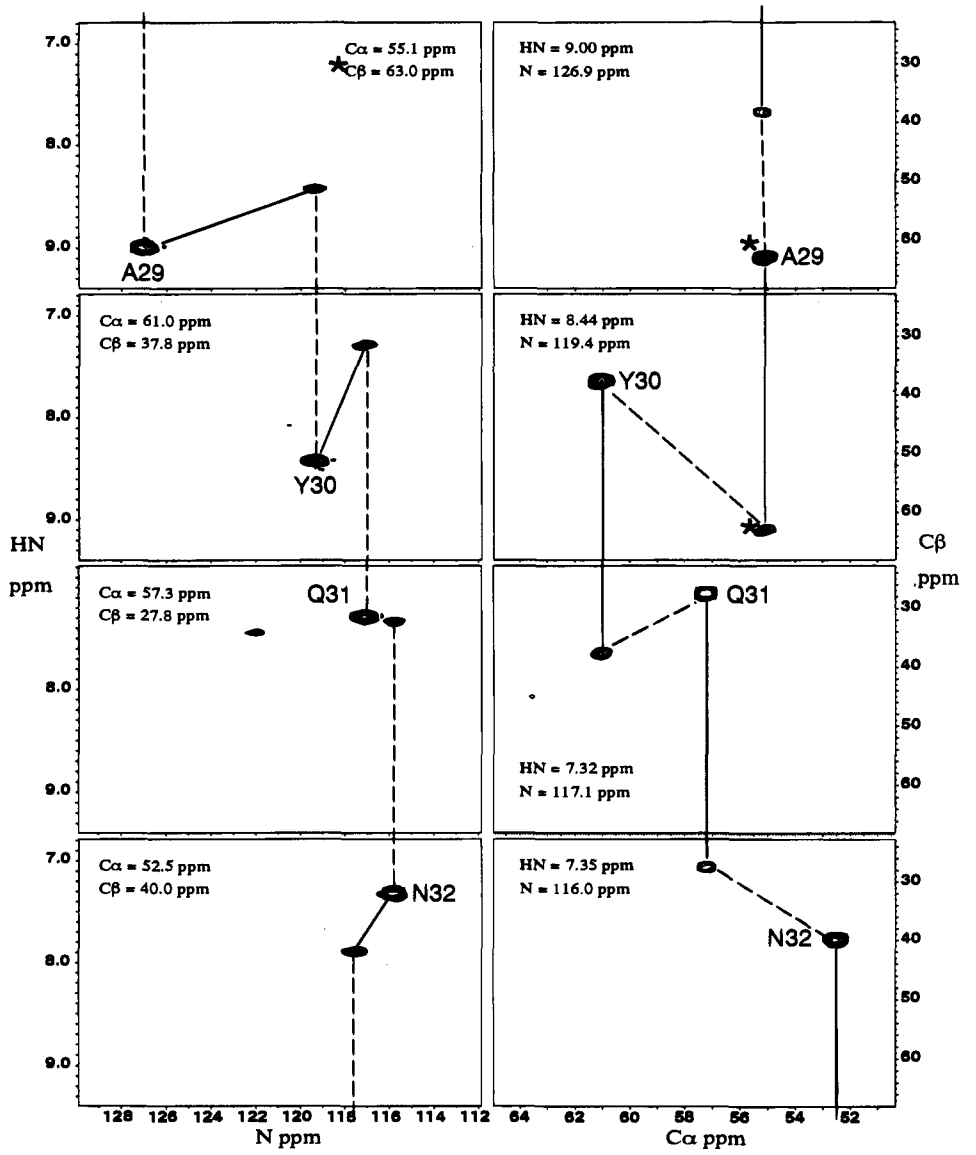

Figure 8. Selected planes from the 4D HNCACB experiment at ($^{13}C^{\alpha}$, $^{13}C^{\beta}$) and (^{15}N, HN) chemical shifts of residues A29–N32. The corresponding chemical shift pairs are indicated in the upper corner of each 2D data set. Note that A29 (*) is folded in the $^{13}C^{\beta}$ dimension and the actual $^{13}C^{\beta}$ chemical shift is 16.8 ppm. Although not indicated in the figure, all peaks folded in this dimension are of opposite sign relative to correlations that are not folded since a first-order phase correction of 180° is employed in the $^{13}C^{\beta}$ dimension.

proteins, it may be advantageous to increase the dimensionality of experiments from three to four so that linkages of $^{13}C^{\alpha}$, $^{13}C^{\beta}$, ^{15}N, and HN chemical shifts can be provided from a single cross peak in the 4D spectrum. It is strightforward to convert the 3D HN(COCA)CB and HN(CA)CB experiments illustrated in Figures 2b,c into 4D experiments which record $^{13}C^{\alpha}$, $^{13}C^{\beta}$, ^{15}N, and HN shifts. In this case the two τ_f periods immediately proceding the t_1 evolution periods in the 3D experiments are converted into constant time evolution periods for recording $^{13}C^{\alpha}$ magnetization. Figure 2d illustrates the pulse scheme used for the 4D HNCACB experiment.

Figure 8 shows a number of planes from the 4D HNCACB experiment at particular $^{13}C^{\alpha}$ and $^{13}C^{\beta}$ chemical shifts as well as the corresponding ^{15}N and HN planes. Each of the planes displays both intra- and inter-residue correlations providing a very straightforward approach for sequential assignment. Of course, in the absence of any degeneracies in (^{15}N, HN) and ($^{13}C^{\alpha}$, $^{13}C^{\beta}$) pairs of chemical shifts and assuming a complete data set, the assignment is, in principle, trivial. Often degeneracies can be sorted out by making use of the fact that particular amino acids have distinctive carbon chemical shifts.[37]

In order to quantitate the sensitivity of each of the experiments, the S/N of each cross peak has been measured, and histograms showing the percentage of residues having a defined value of S/N are plotted in Figure 9. An estimate of the signal intensity of each peak was obtained from the peak height (measured using the software PIPP[19]) and the standard deviation in the noise estimated from a region of the spectrum without signal. Almost complete intraresidue correlations were obtained in each of the CT-HNCA, HN(CA)CB, and 4D HNCACB experiments with over 95% of the expected interresidue correlations available from each of these experiments as well. In addition, nearly complete inter-residue correlations were observed in the CT-HN(CO)CA and HN(COCA)CB experiments.

The assignments of HN, ^{15}N, $^{13}C^{\alpha}$, and $^{13}C^{\beta}$ chemical shifts provided by the experiments described above are presented in Table 1. The assignments are consistent for the most part with those reported earlier for the trpR/DNA complex containing the natural corepressor L-tryptophan[38] (5-methyltryptophan is the corepressor in the present study). A number of differences,

(37) Grzesiek, S.; Bax, A. *J. Biomol. NMR* **1993**, *3*, 185.
(38) Zhang, H.; Zhao, D.; Revington, M.; Lee, W.; Jia, X.; Arrowsmith, C. H.; Jardetzky, O. *J. Mol. Biol.* **1994**, *238*, 592.

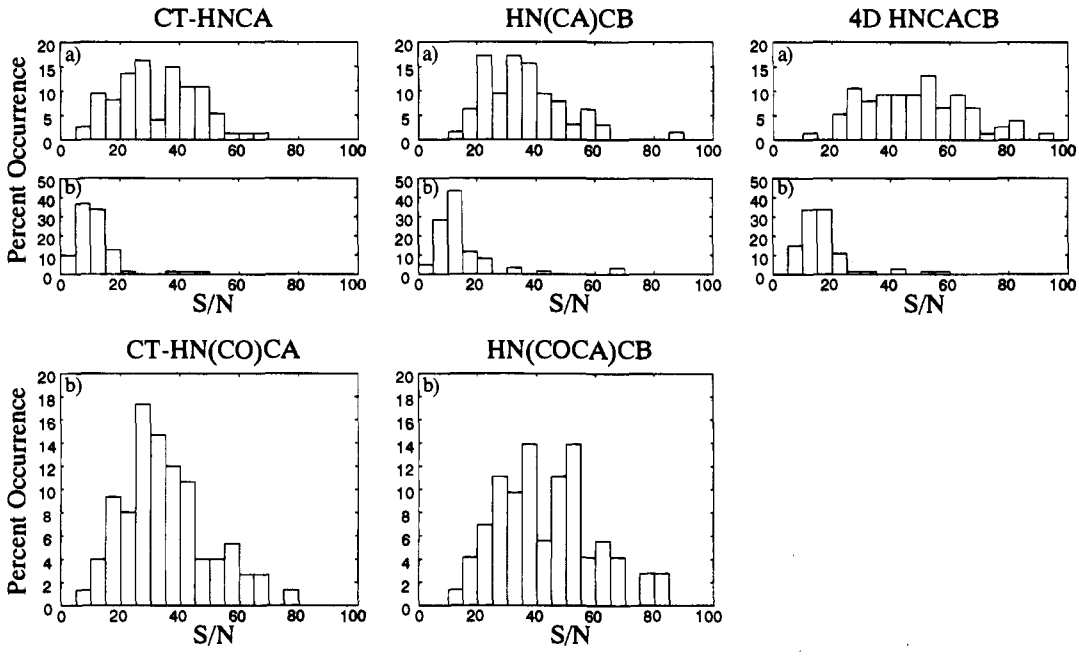

Figure 9. Histograms showing the signal-to-noise (S/N) of intraresidue (a) and interresidue (b) correlations in each of the 3D and 4D data sets. The signal intensity of each cross peak is the interpolated peak height measured using the program PIPP[19] while the rms noise is calculated from a region of each data set which does not contain signal. Overlapped peaks are excluded from the histograms. Some of the peaks from residues 105−108 are off scale (S/N values > 100).

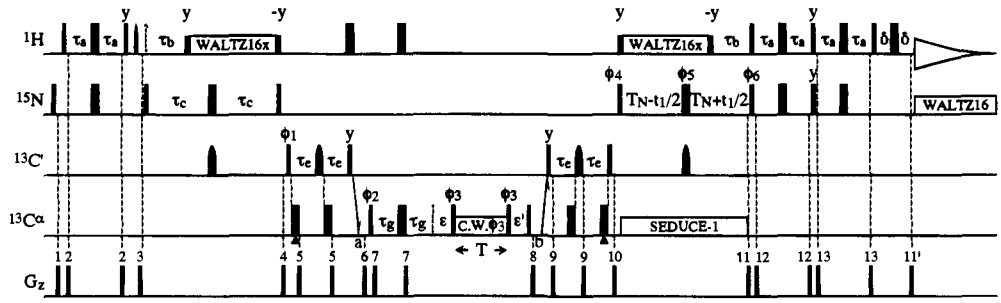

Figure 10. Pulse scheme for the measurement of $^{13}C^{\alpha}$ $T_{1\varrho}$ values for $^{13}C^{\alpha}$−^{2}H spin pairs. The experiment makes use of an HNCOCA transfer of magnetization and is very similar to the scheme of Figure 2a. All of the details of this experiment are identical to what was described for the HN(CO)CA experiment with the following exceptions. The delay τ_g is set to $1/(4J_{HC}) \sim 1.7$ ms so that carbon magnetization associated with $^{13}C^{\alpha}$−$^{1}H^{\alpha}$ pairs becomes antiphase and is not transferred into an observable signal by the remaining pulses in the sequence. In this way $T_{1\varrho}$ values of carbons directly coupled to deuterons only can be measured. The delays ϵ and ϵ' are set according to the relations $\epsilon = 1/(2\pi\nu_1)$ and $\epsilon' = 1/(2\pi\nu_1) - (4/\pi)\tau_{90}$, where ν_1 is the strength of the spin lock field in Hz and τ_{90} is the $^{13}C^{\alpha}$ 90° pulse width.[39] A spin lock field of 1.4 kHz centered at 58 ppm is employed. The phase cycling is $\phi_1 = (x,-x)$; $\phi_2 = 2(x),2(-x)$; $\phi_3 = 4(y),4(-y)$; $\phi_4 = x$; $\phi_5 = 4(x),4(-x)$; $\phi_6 = x$; rec $= (x,-x,-x,x)$. For each value of t_1, N- and P-type coherences are obtained by recording two data sets whereby the sign of the gradient g_{11} is inverted and 180° added to the phase of ϕ_6 for the second data set.[25] The phase of ϕ_4 and the phase of the receiver are incremented by 180° for each increment of t_1.[51] For the measurement of $^{13}C^{\alpha}$ $T_{1\varrho}$ values for $^{13}C^{\alpha}$−^{1}H pairs (i.e., nondeuterated samples), the sequence is identical with the exception that the $2\tau_g$ period is removed. Note that both ^{1}H 180° pulses between the two ^{1}H WALTZ-16$_x$[45] decoupling periodes are removed as well. In this case $\epsilon = \epsilon' = 1/(2\pi\nu_1) - (4/\pi)\tau_{90}$ and ^{1}H 180° pulses are applied every 2 ms to minimize the effects of cross correlation between CSA and dipolar relaxation mechanisms.[52,53] Note that the ^{1}H 180° pulses are applied in pairs with alternating phases (i.e., $[180_x$ 2 ms 180_{-x} 2 ms$]_n$) to ensure that water is along the $+z$ axis at the end of the spin lock period.

however, are deserving of discussion. First, of the 411 HN, ^{15}N, $^{13}C^{\alpha}$, and $^{13}C^{\beta}$ chemical shifts reported here, 61 were previously unassigned and 29 of the tentative assignments in ref 38 have been obtained with certainty using the present set of experiments. A total of 27 chemical shifts in Zhang *et al.*[38] are significantly different from values measured in our spectra; 12 of these were reported as tentative and are concentrated in regions that suffer from broad line widths and/or conformational averaging in the complex with the natural corepressor (residues 47−49, 56, 67, and 68). Many of the remaining 15 differences in shifts are from residues concentrated in the ligand-binding pocket (residues 43, 54, 57, 83, 85, and 86) and are likely due to real differences between the two complexes.

In order to determine the actual gains in carbon relaxation times associated with deuteration, we have measured $^{13}C^{\alpha}$ $T_{1\varrho}$ values in the trpR complex by making use of an HNCOCA transfer of magnetization from the HN of a given residue to the $^{13}C^{\alpha}$ of the previous residue. After a spin lock period the magnetization is transferred back to the HN proton for detection. In this way $^{13}C^{\alpha}$ $T_{1\varrho}$ values can be measured indirectly from a series of ^{15}N−HN correlation maps recorded with different spin lock times. The pulse sequence that has been used is indicated in Figure 10 with a scheme to eliminate contributions from the population of molecules with $^{13}C^{\alpha}$ spins one-bond coupled to ^{1}H and not ^{2}H.[13] The approach that we have taken for measuring $T_{1\varrho}$ values eliminates the offset dependence which would normally accompany the projection of carbon transverse magnetization onto the effective field produced by the combination of the spin lock field and the residual Zeeman field.[39] Note that during the spin lock period the magnetization of interest is

(39) Yamazaki, T.; Muhandiram, R.; Kay, L. E. *J. Am. Chem. Soc.* **1994**, *116*, 8266.

Table 1. HN, ^{15}N, $^{13}C^{\alpha}$, and $^{13}C^{\beta}$ Chemical Shifts for Trp-Repressor Complex at 37 °C

residue	NH	^{15}N	$^{13}C^{\alpha}$	$^{13}C^{\beta}$	residue	NH	^{15}N	$^{13}C^{\alpha}$	$^{13}C^{\beta}$
A2[a]			52.0	18.5	R56	7.44	122.00	57.5	28.0
E3	8.58	122.38	55.3	28.6	I57	8.22	119.00	66.0	36.8
E4	8.48	122.38	55.0	29.0	V58	8.03	118.38	67.1	30.7
S5	8.44	119.19	55.8	63.0	E59	8.48	117.50	59.5	29.0
P6	----	-----	63.0	31.0	E60	8.42	113.93	56.6	28.2
Y7	8.00	119.75	57.5	38.0	L61	9.07	124.44	57.2	40.0
S8	7.90	117.88	58.0	63.5	L62	8.03	118.42	56.2	41.0
A9	8.52	126.50	53.8	17.5	R63	8.31	119.56	58.6	29.6
A10	8.10	121.25	53.5	17.7	G64	7.51	102.12	46.2	----
M11	7.90	118.81	56.2	31.5	E65	7.89	119.19	56.7	31.0
A12	8.09	123.31	54.3	17.7	M66	8.58	119.07	54.6	35.0
E13	8.15	119.38	58.1	28.3	S67	8.85	118.86	56.8	64.0
Q14	8.20	119.75	59.0	29.0	Q68	9.37	120.85	60.5	25.7
R15			58.1	28.0	R69	8.41	117.69	59.0	29.0
H16	8.40	120.50	58.5	27.0	E70	7.63	120.31	58.5	28.7
Q17	8.20	122.75	58.8	28.0	L71	8.43	122.75	57.1	41.0
E18			(57.7)[b]	(28.8)[b]	K72	8.28	119.56	59.2	29.6
W19	8.03	123.13	58.0	28.4	N73	7.64	118.62	55.1	37.8
L20	7.80	117.50	56.9	39.2	E74	8.20	121.44	58.1	28.4
R21	7.90	120.88	58.9	28.5	L75	7.78	113.94	54.1	42.0
F22	8.02	121.25	61.0	36.6	G76	7.96	110.94	46.2	----
V23	7.84	119.75	65.4	30.2	A77	7.41	118.81	49.2	21.2
D24	7.92	121.63	56.5	40.8	G78	9.56	106.44	43.8	----
L25	8.16	124.29	57.2	41.2	I79	9.59	129.12	61.5	37.3
L26	8.34	119.88	56.5	39.0	A80	9.22	122.75	53.6	18.4
K27	7.31	120.83	59.2	31.5	T81	7.69	119.38	64.8	68.0
N28	7.56	116.78	55.2	38.0	I82	7.20	122.56	63.8	34.5
A29	8.99	126.92	55.1	16.8	T83	8.82	119.38	65.8	68.0
Y30	8.42	119.38	61.1	37.2	R84	8.18	122.94	59.2	28.2
Q31	7.30	117.15	57.2	27.5	G85	7.91	110.83	48.2	----
N32	7.32	115.73	52.5	40.3	S86	8.75	117.83	59.8	62.5
D33	7.89	117.54	55.8	39.5	N87	9.03	117.47	55.2	37.0
L34	8.22	118.36	53.0	42.0	S88	8.05	118.63	62.4	62.1
H35	9.06	121.15	58.6	28.0	L89	8.54	124.60	57.3	41.0
L36	7.47	119.43	59.1	36.4	K90	8.02	118.45	58.9	31.7
P37	----	-----	64.7	30.0	A91	7.01	118.17	51.0	18.2
L38	7.95	120.01	58.0	41.0	A92	7.43	123.88	49.8	17.0
L39	8.91	120.90	57.8	40.5	P93	----	-----	61.9	31.2
N40	8.16	118.60	54.1	37.2	V94	8.85	125.00	65.2	30.8
L41	7.67	120.09	57.2	41.2	E95	9.71	119.19	59.2	27.6
M42	8.57	115.30	55.1	31.0	L96	7.23	117.69	56.5	41.0
L43	7.67	115.70	53.2	44.1	R97	7.91	119.75	60.2	29.1
T44	9.80	117.88	58.6	67.1	Q98	8.71	116.19	58.2	27.8
P45	----	-----	65.1	30.8	W99	7.42	121.44	61.2	28.0
D46	8.16	116.75	56.7	38.5	L100	8.83	117.88	57.0	41.6
E47	8.63	118.63	58.2	29.0	E101	7.96	116.94	59.1	28.5
R48	7.66	117.13	59.8	29.0	E102	7.40	118.44	58.2	27.8
E49	7.61	117.01	58.8	28.8	V103	7.91	113.75	63.6	31.0
A50	8.10	122.29	54.5	16.5	L104	8.27	117.88	55.5	41.5
L51	8.00	119.05	57.8	40.1	L105	7.03	115.62	54.2	40.0
G52	8.09	106.30	46.4	----	K106	7.17	119.94	55.8	32.0
T53	7.90	120.13	66.2	68.0	S107	8.22	118.06	57.5	63.8
R54	8.20	119.75	60.0	29.4	D108	7.96	127.81	55.1	41.4
V55	8.11	118.63	65.5	30.3					

[a] ~90% of the amino-terminal methionine of the original trpR translation product is removed.[54] [b] Tentative assignment.

of the form $4C_x^{\alpha}C_z'N_z$, where C_x^{α} is the transverse component of $^{13}C^{\alpha}$ magnetization and C_z' and N_z are the z components of carbonyl and nitrogen magnetization, respectively. To a good first approximation the measured relaxation rate of $4C_x^{\alpha}C_z'N_z$ is given by

$$1/T_{1\varrho}^{\text{measd}} = 1/T_{1\varrho}^{C^{\alpha}} + 1/T_1^{C'} + 1/T_1^{N} \quad (1)$$

where $T_{1\varrho}^{\text{measd}}$ is the value measured in the experiment, $T_{1\varrho}^{C^{\alpha}}$ is the actual $T_{1\varrho}$ value of the $^{13}C^{\alpha}$ spin of residue $(i-1)$, $T_1^{C'}$ is the selective T_1 value of the carbonyl spin of residue $(i-1)$, and T_1^{N} is the ^{15}N T_1 value of residue i. Therefore, in order to extract $^{13}C^{\alpha}$ $T_{1\varrho}$ values from this experiment, it is necessary to measure $^{13}C'$ and ^{15}N T_1 values as well. In a previous study[39] we have measured the selective carbonyl $1/T_1$ rate in alanine dissolved in glycerol at 10 °C (correlation time of 16.7 ns) and obtained a value of 0.55 s^{-1}. The dominant contribution to the selective $1/T_1$ rate is from $^{13}C^{\alpha}-^{13}C'$ spin flips which scale as the overall correlation time. For the case of the trpR complex an overall correlation time of 14.5 ± 0.9 ns is estimated on the basis of ^{15}N T_1/T_2 ratios obtained from 36 residues that reside in well-structured regions of the molecule. Therefore an approximate value of 0.5 s^{-1} ((14.5/16.7) × 0.55 s^{-1}) is estimated for $1/T_1^{C'}$ in the case of trpR. In contrast, the average value of $1/T_1^{N}$ was measured to be 1.2 s^{-1} for trpR. Since $1/T_{1\varrho}^{C^{\alpha}} > 1/T_1^{N} > 1/T_1^{C'}$ (see Figure 1), we have elected to measure T_1^{N} on a per residue basis and assume a uniform value of 0.5 s^{-1} for $1/T_1^{C'}$ in the calculation of $1/T_{1\varrho}^{C^{\alpha}}$ from $1/T_{1\varrho}^{\text{measd}}$. The $T_{1\varrho}^{C^{\alpha}}$ values are converted to T_2 values via the relation[40]

$$1/T_{1\varrho} = \sin^2\theta\,(1/T_1) + \cos^2\theta\,(1/T_2) \sim \cos^2\theta\,(1/T_2) \quad (2)$$

where $\theta = \tan^{-1}\{\Delta\omega^i/(\gamma B_1)\}$, $\Delta\omega^i$ is the offset of $^{13}C^{\alpha}$ spin i from the carrier, and γB_1 is the strength of the spin lock field. Equation 2 assumes that $J(\gamma B_1) \sim J(0)$, where $J(\omega)$ is the spectral density function describing the motion evaluated at ω.

Representative $T_{1\varrho}$ decay curves for both deuterated and protonated samples are indicated in Figure 11a,b. Figure 11c compares $^{13}C^{\alpha}$ T_2 values of the fully protonated trpR sample with T_2 values of the 70%-deuterated sample where the contributions from the population of molecules with $^{13}C^{\alpha}$ spins one-bond coupled to ^1H are eliminated. An average value for T_2 of 130 ± 12 ms is obtained for the deuterated sample versus 16.5 ± 3.0 ms for the fully protonated sample. A T_2 value of 16.5 ms agrees well with the value predicted for a molecule undergoing isotropic motion with a correlation time of 14.5 ns. (see Figure 1). However, the measured average $^{13}C^{\alpha}$ T_2 value of 130 ms for $^{13}C^{\alpha}-^{2}H$ pairs in the trpR complex is considerably lower than would be predicted assuming that the relaxation of the carbon spin is due exclusively to dipolar interactions with the attached deuteron. In this case a T_2 value of approximately 250 ms is predicted. If one includes contributions to the relaxation of the $^{13}C^{\alpha}$ spin from the adjacent carbonyl and $^{13}C^{\beta}$ and ^{15}N spins as well as CSA contributions (assuming an anisotropy of $\Delta\sigma = 34$ ppm[41]), a $^{13}C^{\alpha}$ T_2 value of ~160 ms is calculated. In addition, contributions to relaxation can also arise from neighboring (nonbonded) ^1H dipolar interactions. For example, relaxation from a single $^1H^{\beta}$ proton would decrease the $^{13}C^{\alpha}$ T_2 value to ~135 ms.

Although deuteration of proteins as a vehicle for increasing the molecular mass limitations of current NMR methods has obvious benefits, it is not without problems. Aside from the obvious drawback associated with recording $^1H-^1H$ NOE spectra on molecules with a depleted set of ^1H spins, the substitution of deuterons for protons results in an increase in

(40) Peng, J. W.; Wagner, G. *J. Magn. Reson.* **1992**, *98*, 308.
(41) Naito, A.; Ganapathy, S.; Akasaka, K.; McDowell, C. A. *J. Chem. Phys.* **1981**, *74*, 3190.
(42) Henry, E. R.; Szabo, A. *J. Chem. Phys.* **1985**, *82*, 4753.
(43) Morris, G. A.; Freeman, R. *J. Am. Chem. Soc.* **1979**, *101*, 760.
(44) McCoy, M.; Mueller, L. *J. Am. Chem. Soc.* **1992**, *114*, 2108.
(45) Shaka, A. J.; Keeler, J.; Frenkiel, T.; Freeman, R. *J. Magn. Reson.* **1983**, *52*, 335.
(46) Kay, L. E. *J. Am. Chem. Soc.* **1993**, *115*, 2055.
(47) Boyd, J.; Scoffe, N. *J. Magn. Reson.* **1989**, *85*, 406.
(48) Patt, S. L. *J. Magn. Reson.* **1992**, *96*, 94.
(49) Geen, H.; Freeman, R. *J. Magn. Reson.* **1991**, *93*, 93.
(50) McCoy, M.; Mueller, L. *J. Magn. Reson.* **1992**, *98*, 674.
(51) Marion, D.; Ikura, M.; Tschudin, R.; Bax, A. *J. Magn. Reson.* **1989**, *85*, 393.
(52) Kay, L. E.; Nicholson, L. K.; Delaglio, F.; Bax, A.; Torchia, D. A. *J. Magn. Reson.* **1992**, *75*, 699.
(53) Palmer, A. G.; Skelton, N. J.; Chazin, W. J.; Wright, P. E.; Rance, M. *Mol. Phys.* **1992**, *97*, 359.
(54) Joachimiak, A.; Kelley, R. L.; Gunsalus, R. P.; Yanofsky, C.; Sigler, P. B. *Proc. Natl. Acad. Sci. U.S.A.* **1983**, *80*, 668.

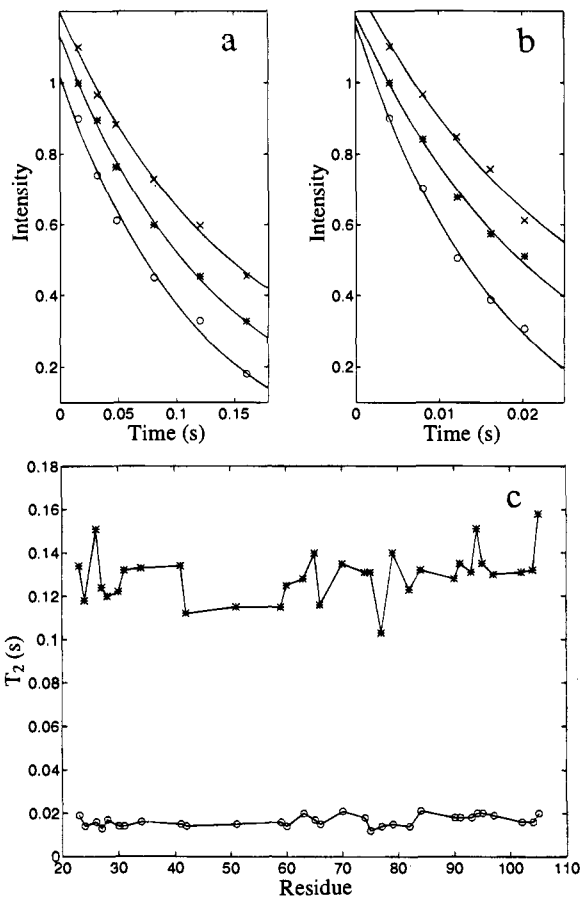

Figure 11. Comparison of $^{13}C^{\alpha}$ transverse relaxation times for $^{13}C^{\alpha}$—^{2}H pairs in the ^{15}N, ^{13}C, ^{2}H trpR complex relative to $^{13}C^{\alpha}$—^{1}H pairs in the ^{15}N, ^{13}C trpR complex. (a) Fits of $T_{1\varrho}$ data measured with the sequence of Figure 10 for $^{13}C^{\alpha}$—^{2}H pairs of residues E65 (O), A91 (×), and L105 (*). (b) Corresponding fits of $T_{1\varrho}$ data for residues in the fully protonated sample. In order to minimize overlap of the decay curves, 0.1 has been added to the intensities of the peaks from A91 while 0.1 has been subtracted from the intensities of peaks associated with E65. (c) Comparison of T_2 values as a function of residue in deuterated (*) and protonated (O) trpR. T_2 values were calcualted from $T_{1\varrho}$ measurements using eqs 1 and 2, with the simplification that $1/T_{1\varrho} \sim \cos^2\theta\,(1/T_2)$. Average T_2 values of 130 and 16.5 ms are obtained from deuterated and protonated samples, respectively.

the T_1 values of the remaining protons. Since the great majority of NMR experiments developed for protein structure determination, including all of the methods described here, begin with magnetization originating on protons, the lengthening of proton T_1 values can have a significant deleterious effect on the sensitivity of these experiments. The severity of the effect will clearly be dependent on the protein studied as well as the level of deuterium incorporation. For experiments where the magnetization begins on the HN proton (all of the experiments considered in this paper), saturation/dephasing of water magnetization should be particularly avoided so that the water is always in a near-equilibrium state. In this way the water can serve as a rich supply of magnetization through exchange with the labile HN protons, thereby increasing the effective rate at which HN magnetization is restored to equilibrium.[30-32] In order to investigate the increase in relaxation times associated with 70% deuteration in trpR, we have measured HN T_1 values for ^{15}N, ^{13}C, 70% ^{2}H trpR and compared these values with T_1 values measured for a protonated ^{15}N, ^{13}C sample.

Figure 12 illustrates the pulse sequence that was used for the HN T_1 measurements. The 90_y (water selective) spin lock 90_{-y} (water selective) portion of the sequence effectively dephases all of the protein magnetization while restoring the

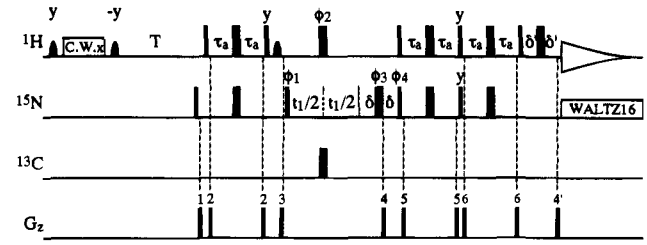

Figure 12. Pulse scheme for the measurement of HN T_1 values. All narrow (wide) pulses have a flip angle of 90° (180°). Unless otherwise indicated the phase of all of the pulses is x. The shaped ^{1}H pulses are either 2 ms 90° rectangular pulses or 2 ms pulses having the SEDUCE-1[44] profile and are selective for water. A 7 kHz C.W. pulse (along the x axis) is applied for 60 ms between the first two shaped pulses to completely randomize ^{1}H magnetization from the protein so that at the start of the recovery period, T, the protein magnetization has the initial condition $M_z = 0$, while for water the magnetization is close to the equilibrium value. ^{15}N decoupling during acquisition is achieved using a 1 kHz WALTZ[45] field, while ^{15}N pulses are applied using a 5.3 kHz field. The carbon 180° pulse is applied using an 18 kHz field centered at 117 ppm, approximately midway between the $^{13}C^{\alpha}$ and the $^{13}C'$ resonances. The delays used are $\tau_a = 2.4$ ms, $\delta = 1.4$ ms, $\delta' = 0.5$ ms. The phase cycling employed is $\phi_1 = x$; $\phi_2 = x,-x$; $\phi_3 = 2(x),2(y),2(-x),2(-y)$; $\phi_4 = x$; rec $= 2(x),2(-x)$. For each value of t_1, N- and P-type coherences are obtained by recording two data sets whereby the sign of the gradient g_4 is inverted and 180° added to the phase of ϕ_4 for the second data set. Data sets obtained for positive and negative g_4 values are stored in separate memory locations and pure absorptive line shapes in the ^{15}N dimension generated by adding and subtracting the N- and P-type data sets, storing the new data sets separately, and applying a 90° zero-order phase correction in the acquisition dimension to one of the new data sets.[25] The phase of ϕ_1 and the phase of the receiver are incremented by 180° for each increment of t_1.[51] The durations and strengths of the gradients (rectangular) are g_1 = (1.0 ms, 8 G/cm), g_2 = (0.5 ms, 8 G/cm), g_3 = (1.5 ms, 15 G/cm), g_4 = (1.25 ms, 30 G/cm), $g_{4'}$ = (0.125 ms, 27.8 G/cm), $g_5 = g_6$ = (0.4 ms, 4 G/cm).

water to the $+z$ axis immediately prior to a delay T, during which time the recovery of protein magnetization occurs. Thus the initial state of the protein magnetization is $M_z = 0$, while the water magnetization is near equilibrium and resides along the $+z$ axis. This is similar to the magnetization state that exists in the triple resonance experiments of Figure 2 at the start of the acquisition period. The remaining portion of the sequence is the enhanced sensitivity HSQC pulse scheme with gradients employed to select for N-type or P-type transfer pathways, described previously.[25] Note that saturation/dephasing of water magnetization is minimized throughout the sequence. Although the relaxation of protons in proteins is a multiexponential process due to cross relaxation with other protons, the recovery curves are nevertheless fit with a single exponential, as Figure 13a,b indicates. A comparison of the HN T_1 values measured for ^{15}N, ^{13}C, 70% ^{2}H and ^{15}N, ^{13}C trpR samples is provided in Figure 13c. On average the HN T_1 values increase by a factor of 1.85 from 0.7 ± 0.2 s to 1.3 ± 0.3 s on deuteration to a level of ~70%.

The results presented clearly indicate that spectra of high sensitivity and resolution can be obtained with ^{15}N, ^{13}C, ^{2}H samples of proteins having molecular masses on the order of 40 kDa. It is also important to establish that these experiments cannot be performed successfully on fully protonated samples. Figure 14 illustrates comparative one-dimensional spectra of fully protonated (a) and ~70% deuterated (b) ^{15}N, ^{13}C labeled trpR recorded using the pulse scheme of Figure 2c, HN(CA)-CB normalized as described in the legend to the figure. In the absence of relaxation effects, the spectra should be of similar intensity. Clearly, this is not the case, and for the most part, only signals from residues of the mobile regions of trpR show

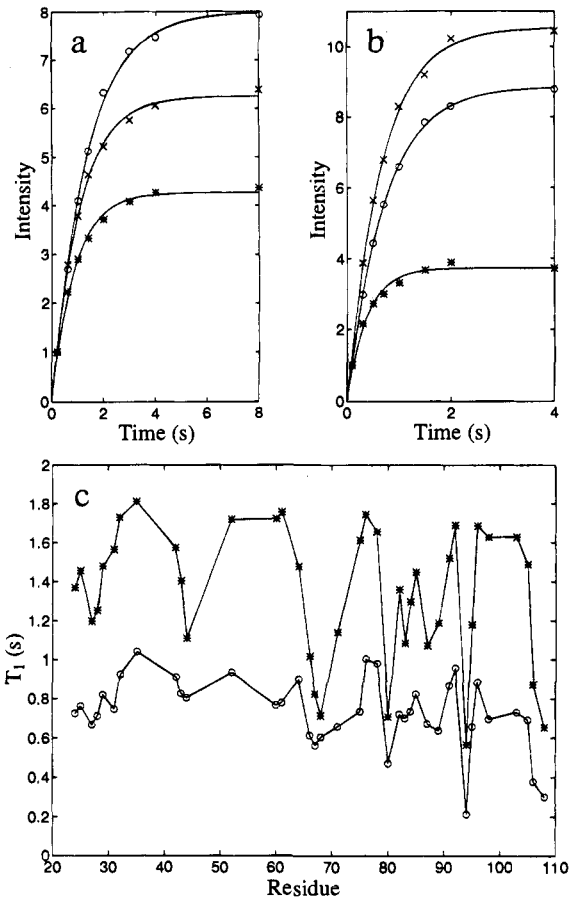

Figure 13. Comparison of HN T_1 values of (a) the ^{15}N, ^{13}C, ~70% ^2H trpR complex and (b) the ^{15}N, ^{13}C trpR complex. Single exponential fits of the recovery data for residues D24 (O), N87 (×), and K106 (*) are shown. (c) HN T_1 values as a function of residue for the deuterated (*) and protonated (O) Trp complexes. Average T_1 values of 1.3 and 0.7 s are obtained for deuterated and protonated samples, respectively.

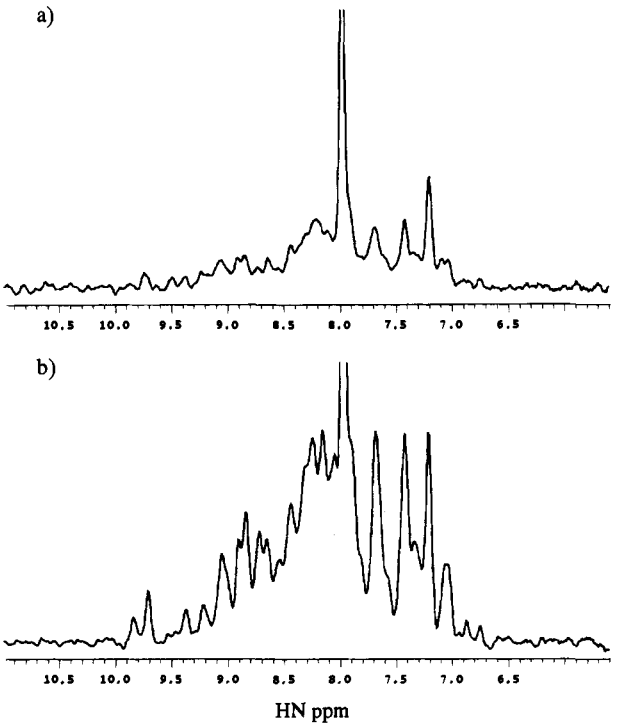

Figure 14. Comparative 1D spectra of fully protonated (a) and ~70% deuterated (b) ^{15}N, ^{13}C trpR using the HN(CA)CB scheme (Figure 2c). A total of 1024 transients were recorded for the ^2H sample and 6928 transients (1024 × 2.6^2) for the ^1H sample which is a factor of 2.6 more dilute. The rms noise levels are normalized in the plots.

significant intensity in the spectrum of the fully protonated sample. It should be noted that equal relaxation delays (2 s) were employed in the recording of both spectra and that the difference in HN T_1 values of a factor of ~1.8 suggests that spectra recorded on the fully protonated sample can be measured using approximately one-half the relaxation delay (1 s) employed in the recording of spectra of the deuterated sample (2 s). Using average NH T_1 values of 1.3 and 0.7 s for the deuterated and protonated samples, respectively, an increase in the relative sensitivity of the protonated spectrum of ~15% can be realized in this case. Nevertheless, the difference in the quality of the spectra is significant, illustrating the importance of deuteration. Because in all of the experiments presented in this paper the time that transverse magnetization resides on the $^{13}C^{\alpha}$ spin is approximately the same (~26–27 ms), similar comparative spectra are obtained with the other pulse schemes as well.

Concluding Remarks

In this paper a number of triple resonance pulse schemes for the assignment of backbone ^{15}N, HN, $^{13}C^{\alpha}$ as well as $^{13}C^{\beta}$ chemical shifts have been presented. The methods have been demonstrated on a ternary complex of ^{15}N, ^{13}C, ~70% ^2H trpR, 5-methyltryptophan, and a 20 basepair trp-operator DNA fragment (MW 37 000). The use of partial deuteration in concert with deuterium decoupling allows exploitation of the long $^{13}C^{\alpha}$ T_2 values, for the case of $^{13}C^{\alpha}-^2H$ pairs, so that high-sensitivity spectra can be obtained. In addition, for CT-HNCA and CT-HN(CO)CA spectra, the use of constant time carbon evolution provides for significant increases in resolution in this dimension relative to previous versions of the experiments. These experiments should provide a useful approach for backbone assignment of many proteins in the 30–40 kDa molecular mass range where experiments such as the HNCACB on fully protonated samples often fail or provide only partial connectivities. Current efforts are directed toward the development of experiments for extending the assignment of all of the side chain ^1H and ^{13}C spins.

Acknowledgment. This research was supported by the National Cancer Institute of Canada (C.H.A and L.E.K), by the National Sciences and Engineering Research Council of Canada (L.E.K), and by the Human Frontiers Science Program (C.H.A). Toshio Yamazaki is the recipient of a Human Frontiers Science Program Fellowship.